Human-induced fire regime shifts during 19th century industrialization: A robust fire regime reconstruction using northern Polish lake sediments

Elisabeth Dietze[1,2]*, Dariusz Brykała[3], Laura T. Schreuder[4], Krzysztof Jażdżewski[5], Olivier Blarquez[6], Achim Brauer[2], Michael Dietze[7], Milena Obremska[8], Florian Ott[9], Anna Pieńczewska[10], Stefan Schouten[4,11], Ellen C. Hopmans[4], Michał Słowiński[12]

1 Alfred-Wegener-Institute Helmholtz Center for Polar and Marine Research, Research Unit Potsdam, Polar Terrestrial Environmental Systems, Potsdam, Germany, 2 GFZ German Research Centre for Geosciences, Section Climate Dynamics and Landscape Evolution, Potsdam, Germany, 3 Polish Academy of Sciences, Institute of Geography and Spatial Organization, Toruń, Poland, 4 Royal Netherlands Institute for Sea Research, Department of Marine Microbiology and Biogeochemistry, and Utrecht University, Texel, The Netherlands, 5 Museum of the Kościerzyna Land, Kościerzyna, Poland, 6 Département de Géographie, Université de Montréal, Montréal, Québec, Canada, 7 GFZ German Research Centre for Geosciences, Section Geomorphology, Potsdam, Germany, 8 Polish Academy of Sciences, Institute of Geological Sciences, Warsaw, Poland, 9 Max Planck Institute for the Science of Human History, Department of Archaeology, Jena, Germany, 10 Kazimierz Wielki University, Institute of Geography, Bydgoszcz, Poland, 11 Faculty of Geosciences, Utrecht University, Utrecht, The Netherlands, 12 Polish Academy of Sciences, Institute of Geography and Spatial Organization, Warsaw, Poland

* edietze@awi.de

Abstract

Fire regime shifts are driven by climate and natural vegetation changes, but can be strongly affected by human land management. Yet, it is poorly known how humans have influenced fire regimes prior to active wildfire suppression. Among the last 250 years, the human contribution to the global increase in fire occurrence during the mid-19th century is especially unclear, as data sources are limited. Here, we test the extent to which forest management has driven fire regime shifts in a temperate forest landscape. We combine multiple fire proxies (macroscopic charcoal and fire-related biomarkers) derived from highly resolved lake sediments (i.e., 3–5 years per sample), and apply a new statistical approach to classify source area- and temperature-specific fire regimes (biomass burnt, fire episodes). We compare these records with independent climate and vegetation reconstructions. We find two prominent fire regime shifts during the 19th and 20th centuries, driven by an adaptive socio-ecological cycle in human forest management. Although individual fire episodes were triggered mainly by arson (as described in historical documents) during dry summers, the biomass burnt increased unintentionally during the mid-19th century due to the plantation of flammable, fast-growing pine tree monocultures needed for industrialization. State forest management reacted with active fire management and suppression during the 20th century. However, pine cover has been increasing since the 1990s and climate projections predict increasingly dry conditions, suggesting a renewed need for adaptations to reduce the increasing fire risk.

Introduction

Fire has influenced global biogeochemical cycles and natural ecosystems since the late Silurian [1, 2] and has been essential to human evolution since at least the early Pleistocene [1, 3]. Humans have used fire for large-scale land cover control [4–6], which may have affected fire regimes and the atmospheric composition beyond their natural variability over the past several millennia [7–10]. In light of increasing drought occurrence and fire risks due to global climate and land management change [11, 12], it is necessary to consider past climate-human-fire relationships that provide the baseline for current and future adaptation strategies. A key period in shaping modern and future human-fire relations is the 18th and 19th centuries CE [13, 14], when one of the largest socio-ecological transitions in human history—industrialization—significantly altered land use strategies due to rapidly growing population densities and energy demands, with fire becoming less important as a land management tool but rather turned into a threat [3–5].

Global sedimentary charcoal records [15–17] and fire-related CO and CH_4 concentrations in Antarctic ice cores [18, 19] show that biomass burning peaked during the mid-to-late 19th century and subsequently declined. This increase in fire was mainly attributed to improvement of natural burning conditions at the end of the Little Ice Age (i.e., a warmer, drier climate and increased biomass availability), but also to increased rates of human land-cover change [15, 20–24], with the intentional use of fires to expand grass and agricultural land [25] and in forest management [26]. During the late 19th to early 20th century, both fire occurrence and the area burnt strongly decreased in industrialized areas independent of spatial scale; this is generally attributed to fire suppression due to the reduced importance of fire for human livelihoods [5, 22, 27]. The initiation of fire suppression is mainly associated with thresholds in population densities and landscape fragmentation induced by the expansion of cropland and pastures [14, 28]. Due to fuel accumulation, fire suppression represents a major factor contributing to increasing modern and future fire risks, not only in fire-prone landscapes [29, 30].

Assessment of the reconstructed decadal-scale variability of biomass burning using dynamic vegetation-fire models has revealed a lack in understanding of past fire regimes and emissions [14, 28] for two reasons. First, models based on modern global fire emission data include highly resolved fire regime parameters and burning emission factors [14, 31] that are largely unknown for periods preceding instrumental data [32]. Second, past human—fire—land-use relationships are highly uncertain regarding the relative importance of ignition, suppression, and human impacts on fire regimes, especially during periods predating active fire suppression [14, 33, 34]. These unknowns challenge the capability to reliably predict future fire regime shifts and to adapt to projected increased fire risks.

Guiding future carbon cycle modeling, land management, and nature conservation efforts requires a comprehensive understanding of past fire regimes (i.e., the characteristic frequency, severity, intensity, and seasonality of fire over space and time) combined with information on past (human) land cover and climatic changes [4, 25, 26, 32]. Fire intensity, the rate of energy released per unit fire line (kW m-1) related to burning temperatures and durations, i.e. fire residence time [35], determines combustion efficiency and the severity of impacts on ecosystems, and varies with fuel moisture, rate of spread, and fire type (e.g., surface vs. crown, smoldering vs. flaming fire) [35–37]. Combined with the amount and type of biomass burnt, fire intensity determines the injection height of the smoke plume [38, 39] and absolute emission factors needed to assess the role of fires in biogeochemical cycles [37, 40].

To characterize past fire regimes, fire frequencies and the area and amount of biomass burnt can be reconstructed using sedimentary macrocharcoal (i.e., >150 µm) [41], assuming that larger particles derive from more proximal fires [42–45]. Charcoal, however, provides

little information on fire intensities. In atmospheric chemistry, novel molecular markers used to trace biomass burning of low intensities are the monosaccharide anhydrides (MAs) levoglucosan (LVG, 1,6-anhydro-β-D-glucopyranose) and its isomers mannosan (MAN, 1,6-anhydro-β-D-mannopyranose) and galactosan (GAL, 1,6-anhydro-β-D-galactopyranose). These thermal dehydration products of cellulose (LVG) and hemicellulose (MAN, GAL) form at burning temperatures <350°C, thus representing smoldering conditions [46, 47]. Production ratios between MA isomers are mainly related to the type of biomass burnt, i.e., the taxa-specific composition of (hemi-)cellulose [48], burn duration, and the relative contributions of flaming and smoldering phases [49–51]. MAs have shown potential as sedimentary proxies [36, 41, 52–54], because LVG is stable in the atmosphere for several hours to days [55, 56] and is transported attached to aerosols, e.g., charcoal particles [57]. In temperate soils, MA degradation is substantial [58], whereas LVG hardly degrades in the marine water column and only partly in marine surface sediment [59], suggesting that MAs are stable during and after sedimentation in lakes, similar to charcoal [43].

Here, we test the extent to which forest management drove fire activity over the last 250 years. We characterize and quantify source-area specific fire intensities and relative fire sizes as major parameters of fire regimes near an Old-World center of industrialization in the temperate central European lowlands. We use sub-decadal records of macroscopic charcoal (CHAR, in three size fractions) and MAs from the same samples in a varved sediment core of Lake Czechowskie (Tuchola forest, north Poland), spanning 1640–2010 CE, considering age and proxy uncertainties to obtain statistically robust and spatially and temporally explicit fire regime characteristics. Combined with climate information, quantitative land cover reconstructions from pollen data, and analyses of historical maps and documents, we assess the drivers of changing regional fire regimes and put these in context of anthropogenic influences on globally observed fire activity during the 19th century.

Materials and methods

Study area and sediment coring

The c. 300,000 ha Tuchola forest, north Poland (Fig 1), is characterized by mean annual precipitation and temperature of 570 mm and 7°C during 1951–1980 [60, 61]. Compared to other regions of the world [62], fires are rare and burn small areas (100–250 events per year in Poland, <1 ha per event), occurring mainly during dry summers [63, 64]. Historical documents suggest that a shift in forest management occurred with the first partition of Poland in 1772 CE (Common Era), when northern Poland became Prussian and energy demand for industrialization strongly increased. At the onset of the 18th century, the royal Tuchola forest, as most European forests, was a human-shaped mixed broadleaf forest of reduced carbon stocks [26, 33, 65], due to intensive forest use including charcoal production and fire use to promote heather for beekeeping [66–68]. Yet, a royal decree in 1778 CE and a cabinet order in 1782 CE prohibited the use of fire in forests [69], because forests became main resources for construction wood [67] and state foresters restructured most of the Tuchola forest by planting pine monocultures [26, 69].

Today, c. 90% of the Tuchola forest is covered by single-species, single-aged Scots pine (*Pinus sylvestris*) forest stands with dispersed cropland and pastures [70]. The 77 ha, 32 m deep Lake Czechowskie (53°52′27″N 18°14′12″E, 109 m a.s.l., Fig 1) is located in the northern Tuchola forest in formerly Prussian territory with a historically important route passing north of the lake. The lake's 1970 ha catchment is composed of glacial till and sandy outwash deposits that limit surface runoff and erosion [26, 71, 72].

The sediment core JC11-K5 was recovered in 2011 in 30 m water depth using an UWITEC gravity corer (Fig 1B). Sediments were composed of yellowish-brownish organic and
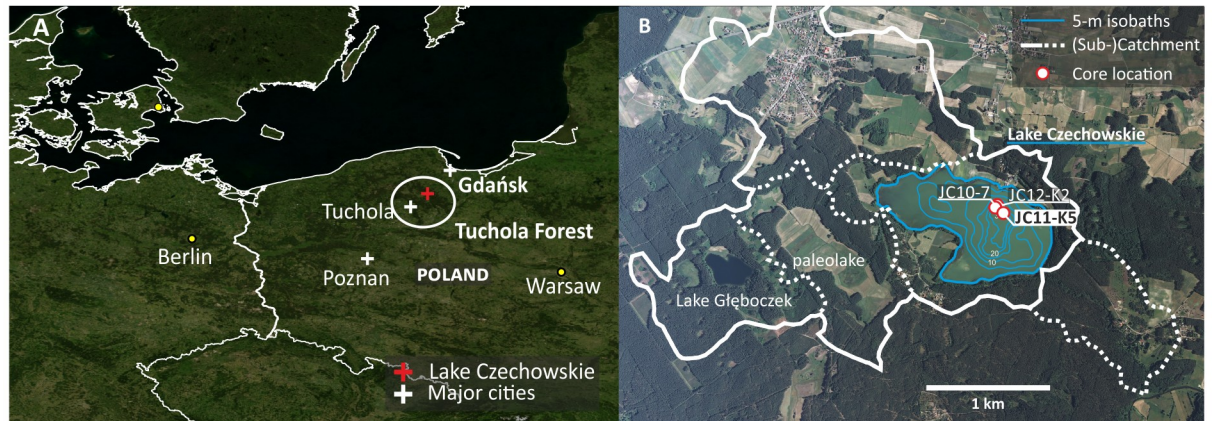
Fig 1. Study area. A) Location of Lake Czechowskie, Tuchola Forest, northern Poland. Map: NASA's Blue marble next generation and state borders by EuroGeographics and UN-FAO. B) The lake catchment, representing the "local scale" referred to in the text, and location of the analyzed sediment core JC11-K5 in the deepest part of the lake. Map: air image provided by provided by Head Office of Geodesy and Cartography, Warsaw, Poland.

https://doi.org/10.1371/journal.pone.0222011.g001

calcareous muds that were finely laminated with dry bulk densities and TOC contents of 0.19 ± 0.03 g cm^{-3} and $7.6 \pm 1.3\%$ ($\mu \pm \sigma$), respectively. Laminations represent calcite varves interrupted by two faintly varved intervals during the mid-20th century, allowing high-resolution reconstruction [72]. JC11-K5 was dated by correlating ten macroscopically visible layers with counted annual layer sequences of adjacent cores (Fig 2). Varve counting of JC12-K2 was performed below the depth of tephra shards at 33 cm related to the Askja eruption in 1875 CE (Fig 2A). As a conservative estimate, we assigned a 2σ error of 10 years to the marker layers that we used for calculating the age-depth model in OxCal v. 4.2, a Bayesian age-depth modelling approach that provides posterior age uncertainties [73]. Prominent shifts in sedimentation rates occurred in c. 1770 and 1890 (Fig 2B) with higher rates related to higher in-lake productivity (thicker diatom layers, such as the marker layer of 1830 CE) and reworking of littoral material (observations from thin sections; F. Ott, unpublished).

Multi-(fire) proxy analyses

For sedimentary macroscopic charcoal analysis, 1 cm^3 of wet sediment was dissolved in water, sieved through a 150-μm mesh. Under a stereomicroscope, macroscopic charcoal of three size classes (150–300, 300–500, and ≥500 μm) was counted continuously throughout the core ($n = 106$, 1630–2011 CE, Fig 2C) assuming the largest charcoal particles to represent flaming fires with nearby source areas [43, 44, 74]. To estimate a proxy error that combines sampling, preparation and macrocharcoal counting uncertainties, we continuously sampled short core JC11-K2 between 35–55 cm core depth (n = 20, Fig 2C), i.e., interval 1840–1875 CE, that could be linked to core JC11-K5 by four marker layers as determined from varve counting. Samples were processed in the same way as for JC11-K5. The numbers of absolute particles cm^{-3} were compared with the JC11-K5 samples of the same time interval (n = 31) to determine an overall mean relative standard deviation of 0.8% (RSD = 100* σ/μ of each sample for all size classes).

To account for low-intensity fires [46], the topmost 75 samples (1780–2010 CE) were also analyzed for MAs ($n = 75$, 1780–2011 CE, Fig 2C): 125–250 mg dry sediment were extracted with a DIONEX Accelerated Solvent Extractor (ASE 200, 100°C, 7.6×10^6 Pa) using a 9:1 solvent mixture of dichloromethane (DCM):methanol (MeOH). As an internal standard, 2.5–5 ng deuterated levoglucosan (dLVG) was added. The total lipid extracts were separated on an
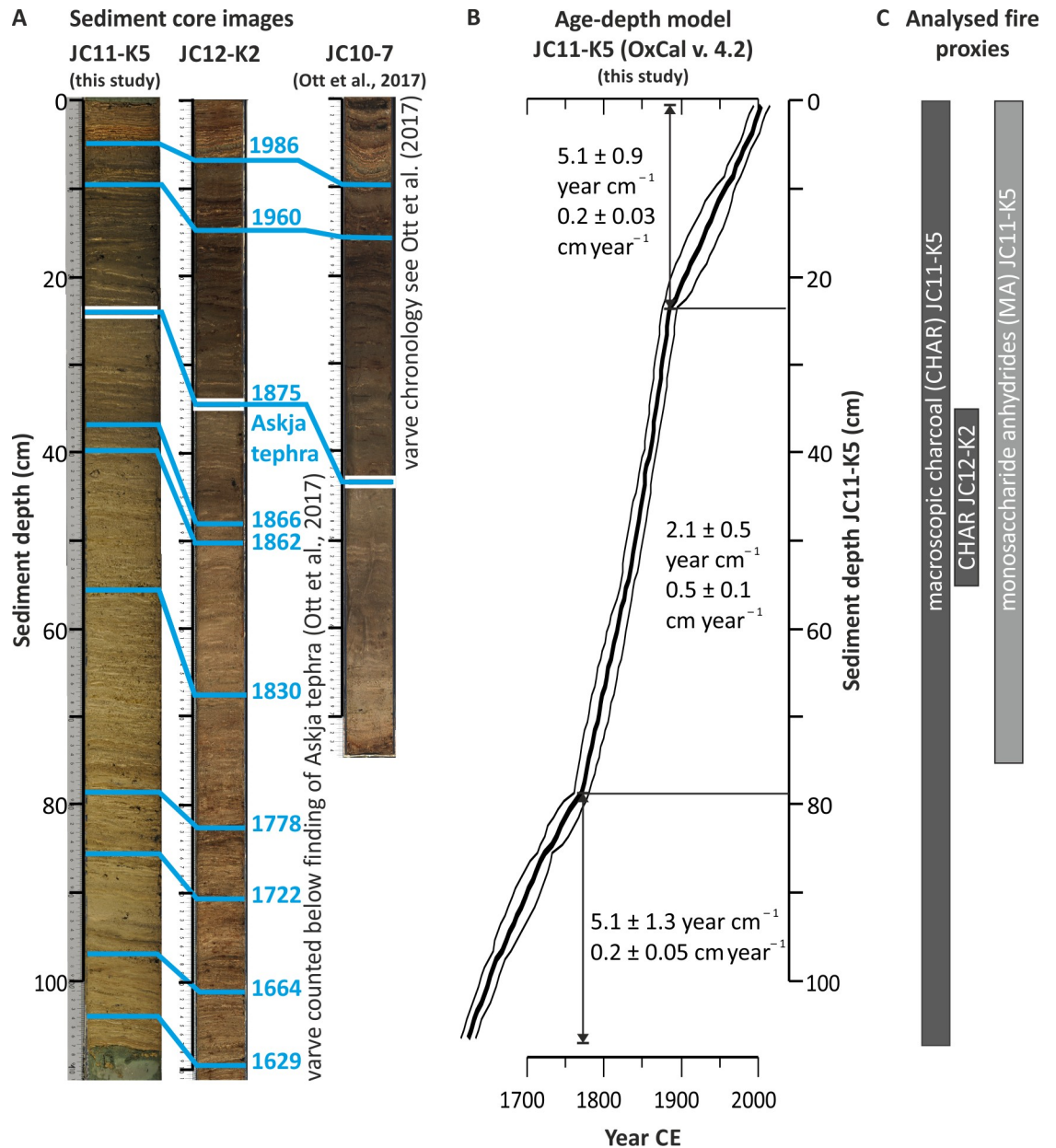
Fig 2. Dating of short core JC11-K5 of Lake Czechowskie. A) Correlation of marker layers (blue) detected in the core image and in short core JC12-K2 (this study) and the core of the master sequence JC10-7 [26, 72]. B) Age-depth model and major changes in sedimentation rates. C) Core sections analyzed for sedimentary charcoal and fire biomarkers.

unactivated SiO$_2$ gel column (Merck Si60, grade 7754) using sequential elution with DCM: MeOH (9:1) and DCM:MeOH (1:1). The 1:1 fractions were re-dissolved in 95:5 acetonitrile: H$_2$O and filtered using a 0.45 µm polytetrafluoroethylene filter before analysis. The MAs were analyzed by ultra-high pressure liquid chromatography-high resolution mass spectrometry using a method adapted from an earlier HPLC-ESI/MS^2 method [75]. Authentic standards for LVG, GAL and MAN were obtained from Sigma Aldrich, and that for dLVG (C$_6$H$_3$D$_7$O$_5$) from Cambridge Isotope Laboratories, Inc. Integrations were performed on mass chromatograms within 3 ppm mass accuracy. Concentrations were corrected for relative response

factors to dLVG of 0.997, 0.822, and 2.137 for LVG, MAN, and GAL, respectively. Instrumental (standard) errors for LVG, MAN, and GAL were 4 ± 3, 14 ± 15, and $28 \pm 38\%$ (1σ), respectively.

Quantitative land cover estimates were derived from pollen records of varve-dated sediment core JC10-7 in 2-cm steps, i.e., at a resolution of ~5 years/sample [26]. To convert % pollen to land cover, we used the REVEALSinR function of the DISQOVER R package with pollen productivity estimates from the PPE.MV2015 data set and the LSM dispersal model [76].

Robust proxy records considering age and proxy uncertainties

We provide a robust Monte Carlo based procedure, which adds uncertainty estimates to the existing charcoal record analysis presented by Blarquez, Girardin [77]. The approach starts with influx calculations of CHAR (particles $cm^{-2}\,a^{-1}$) and MAs (ng $cm^{-2}\,a^{-1}$), which were derived from a Markov chain Monte Carlo routine that we developed in R version 3.4.4 using the base R functions of the stats package (S1 Code, S1 Fig). Sample age ranges are described by a Gaussian function using μ_{age} and σ_{age} of each depth from the marker layer-based OxCal age-depth model. We randomly calculated 10,000 stratigraphically consistent, positive unit deposition time values for each sample (UDT) to retrieve μ_{UDT} and σ_{UDT} of the UDT distribution by UDT (a cm^{-1}) = Δt (a) / Δd (cm) (S1 Code, S1 Fig)

Proxy ranges for each sample are also described by a Gaussian distribution function (μ_{proxy}, σ_{proxy} from parallel measurements) to randomly generate n normally distributed proxy values (PV). These were divided by n randomly generated UDT values (using μ_{UDT} and σ_{UDT}) to yield n flux values: Flux (proxy unit $cm^{-2}\,a^{-1}$) = PV (proxy unit) / UDT (a cm^{-1}). For the flux density function (pdf_{flux}, defined by μ_{flux} and σ_{flux}), we multiplied MA values (ng g^{-1}) by the sample's dry bulk density (g cm^{-3}), excluding extreme values (i.e., values above the 0.99 quantile) that result from combining exceptionally high PVs with exceptionally low UDTs.

To consider the full age uncertainty of a sample, we generated the age density functions pdf_{age} for each sample by combining normalized segments of i) the older tail of the OxCal age distribution for the lower sample boundary, ii) the younger distribution tail for the upper sample boundary, and iii) uniform values between these tails (S1 Code, S1 Fig). Both, pdf_{age} and pdf_{flux} were sampled to generate n likely ages and fluxes per sample (S1 Code). Fluxes that fell into evenly spaced 3-year age bins (i.e., median record resolution, S1 Fig) were used to calculate the output statistics (used in Figs 3 and 4A).

In addition, mean fluxes were calculated using the pretreatment function in the paleofire R package using the default parameters (9) and the mean OxCal age-depth model of core JC11-K5 (Fig 2B, bold line). A comparison showed that robust fluxes were smoothed, but underestimated absolute mean fluxes due to strongly overlapping pdf_{age} of adjacent samples at 1 cm sample resolution. Hence, we averaged the raw proxy and age values of three adjacent samples before robust flux calculation. Median MA flux records were used to calculate MA ratio records (i.e., LVG MAN^{-1} and LVG $(MAN+GAL)^{-1}$) of the same time resolution.

To provide relative estimates of biomass burnt and fire frequencies, fire proxy records were decomposed into a low-frequency background and a high-frequency peak component, a classical approach in sedimentary charcoal analysis [42, 78, 79], which we adopted here also for MA-record analyses. We performed the statistical decomposition in two ways (Fig 3B and 3C). First, CHAR records of the classical influx calculation using the mean age-depth model were decomposed translating some of the main principles of the CHARanalysis program [42] to R (S1 Code). Briefly, charcoal records were interpolated to a 3-year median sample resolution and CHAR was calculated using the pretreatment function in the paleofire R package using
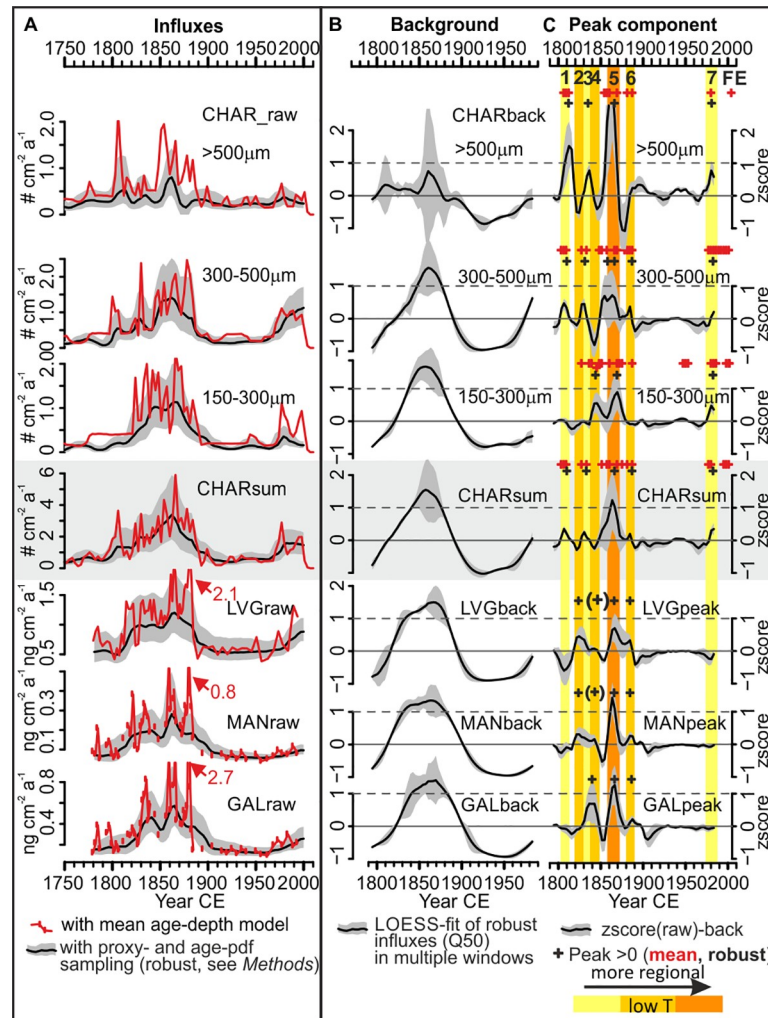
Fig 3. Fire proxy records of Lake Czechowskie, northern Poland. A) Raw macrocharcoal (CHAR, n = 82) and MA (LVG, MAN, GAL, n = 75) influx records. CHAR$_{sum}$ is the summed record of all charcoal particles >150 μm. Black lines and gray polygons are medians and interquartile ranges of robust influx calculations, respectively (*Methods*). Influxes calculated using the classical mean age-depth model are in red. B) Fire proxy background component. Black lines and gray polygons are medians and Q10–Q90 ranges, respectively, of 1,000 random LOESS fits of the standardized median of the robust influx records (black lines in A) with varying window widths. C) Fire proxy peak components. Black lines and gray polygons are medians and Q10–Q90 ranges, respectively, from subtracting the LOESS-fits of B from the standardized median records of A (black lines). Crosses and colored shaded areas (yellow to orange) mark major positive peaks indicating source area- and temperature-specific fire episodes (FEs1–7, Table 1). Black crosses in brackets mark tentative peaks that were above average only for some window widths. Red crosses mark peaks from decomposition of the mean influx record.

the default parameters (9) and the mean OxCal age-depth model of core JC11-K5 (Fig 2B, bold line). A locally-weighted regression smoothing (LOESS) fit with a half window width (hw) of 5% of the entire record length was used to separate the background from the peak component with the R package locfit [80], i.e. Flux$_{peak}$ (proxy unit cm^{-2} a^{-1}) = Flux$_{raw}$−Flux$_{back}$ and Flux$_{back}$ (proxy unit cm^{-2} a^{-1}) = LOESS (Flux$_{raw}$, hw = 0.05). With a Gaussian mixture model (package mixtools [81]), the signal peaks were classified as fire events if they exceeded the 99th percentile of the noise distribution [82, 83]. We attributed closely spaced peaks (of adjacent years) to the same fire episode.
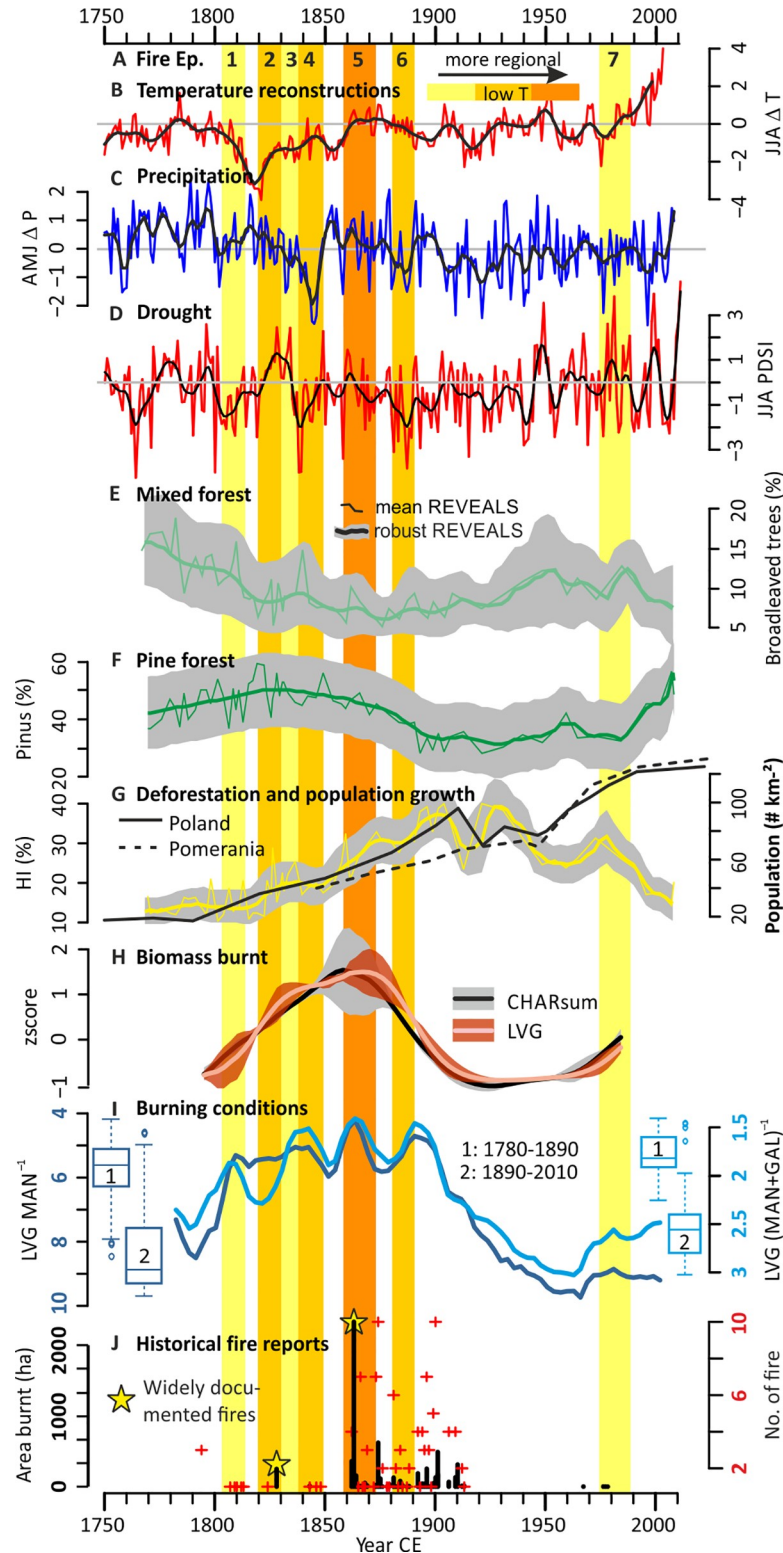
Fig 4. Comparison of fire proxy records with climate, land cover, and historical data. A) Source- and intensity-specific fire episodes (shaded areas from Fig 3C, Table 1); B–C) annual and 20 point LOESS-smoothed June-July-August mean temperatures (JJA Δ T) and April-May-June precipitation (AMJ Δ P) relative to the period 1901–2000 CE [91]. D) Reconstructed Palmer Drought Severity Index (JJA PDSI), reflecting spring-summer soil moisture conditions [92], averaged over the Tuchola area (53.4–54.4˚N, 17.3–18.85˚E, S2 Fig). E–G) REVEALS-transformed

[76] pollen records of the sum of broadleaved taxa (light green), Scots pine (*Pinus sylvestris*, dark green), and human-indicator (HI) taxa (yellow, compared to population densities) from core JC10-7 [26], respectively. Thick lines and gray polygons are medians and Q10–Q90 ranges of the Markov chain Monte Carlo approach (*Methods)*, thin lines are calculated using the classical mean age-depth model. H) Background components of levoglucosan (LVG) and CHAR (CHAR$_{sum}$) from Fig 3B, representing the relative amount of biomass burnt. I) MA ratios representing relative burning conditions (y-axes reversed). J) Minimum estimates of area burnt (ha, black bars) and fire occurrence (red crosses) as reported in historical documents of the Tuchola forest [26] (for 20th century instrumental data see S2 Fig).

https://doi.org/10.1371/journal.pone.0222011.g004

Second, we calculate statistically robust background and peak components following the suggestion of Blarquez, Girardin (77) to vary the window widths during background calculation. Briefly, we standardized the medians of the robust CHAR and MA influx records to get comparable units and distributions. Then, we use a Monte Carlo approach to fit a LOESS in varying window widths (i.e., 5–25% of the record length, comparable to [77], 1000 times randomly sampled) as background and subtracted the 1000 LOESS fits from the medians as 1000 peak component records. We mark the above-average peaks using the Monte Carlo approach that are fewer peaks compared to those derived from classical decomposition using the mean age model and one window width (black vs. red crosses, Fig 3C), the latter classically interpreted as individual fire events considering noise, e.g., related to re-deposition [42, 77].

Here, we assume that fire episodes (FEs) would result in peaks, even when accounting for age and proxy uncertainties, hence, representing periods of multiple fire events that produced sufficiently high influxes of burning residues to be preserved. We use the presence of robust peaks in CHAR and/or MA records (black crosses, Fig 3C) to interpret three types of sub-decadal FEs based on the dominant fire intensity, size, and source area of the burning proxies (Table 1). These are then compared with historically documented fires.

For pollen data, we modified the calculation and used the REVEALS-output ($\mu_{REVEALS}$ and $\sigma_{REVEALS}$) to define the Gaussian distribution function pdf$_{flux}$. For the sum of human indicator taxa (HI, i.e. sum of *Plantago lanceolata, Ceralia spec., Secale spec., Rumex acetosella-var.*), we replaced pdf$_{flux}$ by the summed density functions (pdf$_{sum}$) for each sample generated from *n* sums of randomly drawn REVEALS values of each taxa, allowing only sums ≤100% to sustain realistic land cover percentages.

Historical documents and maps of the Tuchola forest were provided by the State Archives Gdańsk, Bydgoszcz and the State Library and Archive of Prussian Cultural Heritage, Berlin. Many documents were lost and fires were reported sporadically without exact areas measured, especially before 1850 [26, 84]. Hence, documented fire occurrences and extents (Fig 4I and S2 Fig) are minimum estimates, preventing a more quantitative comparison with fire proxy peaks.

Table 1. Classification of robust peaks in fire proxies in relation to fire regime parameters.

Fire intensity	Fire size	Source area	CHAR 150–300	CHAR 300–500	CHAR >500 µm	CHAR sum	Levo-glucosan	Manno-san	Galacto-san
Low-High	Large	Regional	1	1	1	1	1	1	1
High	Small-Medium	Local	1	1	3	3	0	0	0
Low	Medium-large	Regional	1	1	0	0	2	2	2

The number of peaks during the period 1800–2000 (black crosses in Fig 3C) and colours as in Fig 3A. Levoglucosan, mannosan and galactosan are only produced by low fire intensities (more produced if more area burnt). Bigger charcoal pieces are generally linked to more nearby source areas. See text for references and further discussions.

https://doi.org/10.1371/journal.pone.0222011.t001

Results and discussion

Fire regimes during the last two centuries

All fire proxies increase from below average influxes before 1800 CE (e.g., $CHAR_{sum}$: 0.45 particles cm^{-2} a^{-1}, LVG: 0.5 ng cm^{-2} a^{-1}) to maximum influxes during the 1860s ($CHAR_{sum}$: 3.4 particles cm^{-2} a^{-1}, LVG: 1.2 ng cm^{-2} a^{-1}), except the largest CHAR fraction ($CHAR_{>500\mu m}$) that peaks in the early 1800s and during the 1860s (Fig 3A). Influxes then declined to low values by the early 20th century ($CHAR_{sum}$: 0.4 particles cm^{-2} a^{-1}, LVG: 0.5 ng cm^{-2} a^{-1}) and remained low until c. 1970 when $CHAR_{300-500\mu m}$ and LVG influxes increased again until their later peaks ($CHAR_{300-500\mu m}$: 0.8 particles cm^{-2} a^{-1}, LVG: 0.88 ng cm^{-2} a^{-1}) in the 1980s and 2000s, respectively, whereas $CHAR_{>500\mu m}$, MAN, and GAL remained low (median robust influxes, calculated using the Monte Carlo-based approach, Fig 3A).

We find similar decadal-scale background trends for CHAR and MAs ($CHAR_{back}$, MA_{back}, 1780–2010 CE, Fig 3B), which we interpret as relative (not absolute) amount of biomass burnt under various burning conditions and under low temperatures, respectively. $CHAR_{back}$ is known to reflect the regional amount of biomass burnt, although partly affected by sediment reworking and catchment erosion [85, 86]. The latter effect is of limited relevance at Lake Czechowskie as the high sedimentation rates are related to internal productivity [72]. Comparison with the sedimentation rate-independent ratios of the three MA isomers (Fig 4I) shows that MA_{back} (i.e., LVG_{back}, MAN_{back}, and GAL_{back}, Fig 3B) also reflects relative changes in biomass burnt. The MA_{back} and $CHAR_{back}$ records are inversely correlated with the MA ratios (e.g., LOESS-fitted LVG MAN^{-1} vs. $CHAR_{sum\_back}$: r = −0.8, p < 0.001), which are in the range of modern MA emissions and ratios controlled by the type of biomass burnt and burning conditions, i.e. burn duration, and the relative contributions of flaming and smoldering phases [49–51]. The lower MA ratios and their higher variability before 1890 CE than after (boxplots, Fig 4I), with minimum and maximum values during the 1860s and 1960s, respectively (e.g., LVG MAN^{-1}: 4.2 vs. 9.6, Fig 4I) suggests that biomass burning conditions changed significantly in the 20th century.

Yet, the differences between MA_{back} and $CHAR_{back}$ trends suggest varying burning conditions on shorter (sub-decadal) timescales. MA_{back} increased from below average toward 1σ above average anomalies for 15 years longer than $CHAR_{back}$ (1830–1885 vs. 1840–1880 CE, respectively, Fig 3B) and reached maximum anomalies a decade later than $CHAR_{back}$ (c. 1870 and 1860 CE, respectively, Fig 3B), which we attribute to biomass burnt during distinct fire episodes.

Sub-decadal fire episodes (FEs) are marked by distinct peaks in CHAR and/or MA records (black crosses, Fig 3C), with all fire proxies showing higher FE frequencies before than after 1890 CE. CHAR peaks are classically used to reconstruct local fires within ~1 km of the deposit [44, 74], but charcoal can also derive from regional fires within few dozen km [38, 87, 88], e.g., crown fires with high injection columns. Given that charcoal forms under various combustion conditions [43, 44] and MAs represent low burning temperatures (<350˚C) [46, 47], the appearance of peaks in all fire proxies in the 1860s (Table 1, Fig 3C) suggests that during this period fires of all intensities have produced high amounts of residues, probably from local- to regional source areas. Historically, the largest documented fire episode burnt an area of >2300 ha over several parts of the Tuchola forest during August–September 1863 CE within ~25–30 km of Lake Czechowskie (Fig 4I and S2A Fig). The closest documented individual fire was ~14 km northeast (~1250 ha burnt, S2A Fig), probably providing coarser charcoal particles during crown fires with high injection plumes [38].

In addition, comparison of our robust CHAR or MA peaks with historical data [26] suggests the distinction of two further types of FEs (Table 1): local-scale FEs are represented by

three peaks occurring in the coarsest and the total CHAR records during the 1800s, 1830s, and c. 1980 CE, which were not visible in the MA records and only partly in the finer CHAR sizes (FEs 1, 3, 7; Fig 3C, Table 1). We interpret these episodes as small and local, e.g., catchment-scale (Fig 1B), fires that produced limited MAs due to high burning temperatures (Table 1). Such episodes could represent human-induced fires of high intensity with continued fuel supply such as controlled burning of deforestation residues, e.g., after the sale of the lake shore house in the 1980s (Iwiczno Municipality, pers. comm., March 2018).

Low-intensity, regional FEs relate to prominent peaks in the LVG and MAN records during the 1820s that have no equivalent peak in CHAR anomalies, whereas a prominent GAL peak around 1840 CE corresponds to a peak in $CHAR_{150-300 \mu m}$ (FEs 2, 4; Fig 3C). Documented fires of unknown location burnt an area of 250 ha in 1828 CE [89], and fires burnt >10 ha c. 30–40 km southeast of Lake Czechowskie in 1843 CE [26]: these events may be related to the observed MA peaks (Fig 3C). In the 1880s, small MA peaks that are partly reflected in $CHAR_{peak}$ records (FE 6, Fig 3C, Table 1) suggest low-intensity fires corresponding to a fire c. 30 km south of the lake in 1887 (S2 Fig) or to the fires ignited by flying sparks (<130 ha) reported along the Starogard-Chojnice railway line [26, 90] (S2D Fig).

Hence, we can detect low-intensity fire episodes from the sedimentary record and, supported by historical data, specify previously unknown source regions of sedimentary MAs [37, 52–54]. We find that sedimentary MAs derive from a regional source area, within roughly 50 km of the deposit (S2A Fig), recording low-intensity surface or wet-fuel fire events that were large (or long) enough to emit sufficient MAs to be recorded as robust peaks.

Drivers of fire regime shifts

The period 1780–2010 CE is characterized by prominent shifts in fire regimes. Fire episodes and the amount of biomass burnt increased during the early 18th century until the pronounced FE in the 1860s. After this period, the biomass burnt declined until the 1890s towards changed burning conditions and a 70-year-long period without local-to-regional FEs and characterized by below-average biomass burnt. After the 1960s, regional low-intensity fires slightly increased and a local high-intensity FE occurred in the 1980s (Fig 3B and 3C). These decadal-scale regional fire regime trends in the Tuchola forest parallel the observed global biomass burning pattern [14–17] and could, hence, serve as an example to study climate-human-fire relationships that could have contributed to the global pattern. Comparing our source-specific fire regime records with tree ring-derived climate reconstructions, i.e., central European temperature and precipitation [91] and the regional interpolation of the Palmer Drought Severity Index (PDSI) [92] (Fig 4B–4D), quantitative vegetation cover reconstructions from REVEALS-transformed pollen records of the same lake (Fig 4E–4G), and historical documents (Fig 4J and S2 Fig) enables an integrative discussion of the primary drivers climate, human impacts and associated natural vegetation changes.

Climate reconstructions do not show comparable decadal-scale trends (Fig 4B–4D) that would explain the observed trends in biomass burnt and burning conditions (Fig 4I and 4H) with weather and climate only partly explaining fire occurrences and extents here. In temperate forested ecosystems, fires require summer droughts for fuel drying and fire spread [2], which are reported in historical documents [93] and confirmed by PDSI reconstructions for FEs 1, 4, 5 and 6 (Fig 4A and 4D). However, some sub-decadal-scale FEs, including the most prominent FE (i.e., FE 5) and low-intensity FEs as reconstructed using MAs do not relate to prolonged droughts alone (Fig 4A, 4C and 4D), as also reported by Zumbrunnen, Bugmann [94]. The most prominent droughts during the 1800s, 1840s, and 1880s did not result in the largest fire extents (e.g., 1828 and 1863 CE, Fig 4D and 4J), or even no FEs during the minima

in PDSI during the 20th century (Fig 4A, 4C and 4D). This suggests that other factors affecting fire extents and spread act on different timescales that we cannot resolve with the inherent uncertainties in our proxy records.

Modern observations also show that natural ignition by lightning is limited, as strikes occur at low frequencies of <5 flashes km^{-2} a^{-1} [95]. Instead, the historical data that we have analyzed suggest that fire ignition was primarily human-triggered, but not necessarily fully independent of weather and climate (as in Roos, Zedeño [96]). Arson during drought periods as a way to show anti-institutional resentments and unintentional human ignition were reported repeatedly, for example, for widespread fires "by a nefarious hand" in the summer of 1863 CE [26, 84] or along the Starogard-Chojnice steam railway in the 1880s [84, 97], respectively (S2D Fig). Yet, we exclude the intentional use of fire as a human land management tool for three reasons. First, human-indicator taxa from the same lake (HI, i.e., cereals and ruderals, Fig 4G), a proxy for human deforestation, increased two decades after the increases in biomass burning and reached maximum values in the 1930s when biomass burning was already low (Fig 4G and 4H). Second, historical maps confirm the HI trends showing significant extension of open land in the region after the increase in fire (early 20th century). Third, fire was banned as a land management tool by Prussian authorities by the late 18th century (see above).

Instead, we find a link between fire regimes, Scots pine cover, and human forest management, as previously suggested [26]. Pine cover increased by at least 10% since the late 18th century and until reaching a maximum around 1830 CE, then declined by ~20% until c. 1910 CE. This trend precedes a similar trend in biomass burnt during the 19th century by roughly three decades (Fig 4F and 4H). Low MA ratios during the 19th century suggest the burning of softwood, e.g., pine [51], whereas high MA ratios in the 20th century (Fig 4I, axes reversed) indicate either the burning of hardwoods, grasses and crops, or both mixed with burned brown coal emissions [48, 49, 51]. Yet, high ratios are also produced under more flaming conditions and higher burning speeds [51] more typical of grass fires [98]. The lack of local-to-regional FEs (Fig 4A) suggests that 20th-century fires probably occurred outside the Tuchola forest. Hence, we suggest that, here, the co-occurrence of high MA ratios and high HI coverage (Fig 4G and 4I) represents more grassland and crop-residue burning, whereas low ratios suggest pine fires.

Historical documents suggest that forest management was changed strongly after the 1770s, from mixed broadleaved forests towards pine monocultures in the course of industrialization [26, 69]. We suggest that the state decision to use forests solely as a timber resource initiated an unintended socio-ecological adaptive cycle in forest management strategies (sensu Gunderson and Holling [99], Fig 5), superimposed on decadal-scale climate change. Hence, roughly 30 years after the increase in pine cover and decrease of mixed forest (Fig 4E and 4F), single-aged pine stands with heather (Calluna vulgaris) understories [84], i.e. widespread flammable fuel, had grown (phase P2, Fig 5). Supported by some prolonged droughts, biomass burning,
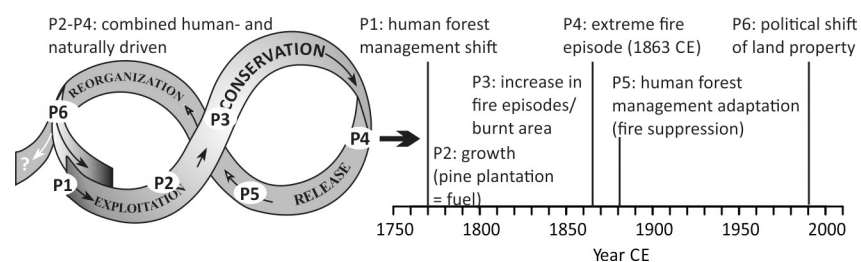

Fig 5. Adaptive cycle of human-induced fire regime shifts during industrialization, including phases P1–6 mentioned in the text (timing for northern Poland). Adapted after Gunderson and Holling [99].

fire occurrence and fire hazard were strongly increasing (Fig 4*A* and 4*H*, P3, Fig 5). Compared to broadleaved trees, pine is easily flammable because of its resin-rich needles and its light canopy that results in rapid drying of its understory, even in rather short dry periods in wet years [2, 94, 100]. During the dry summer of 1863, multiple simultaneous fires spread easily in the Tuchola forest [26] (S2A Fig). Hence, the maximum in CHAR and MA records reflects the regional maximum of available and connected fuel that allowed high fire frequencies and extents, even in wetter years (Fig 4*A, 4D, 4F and* 4*H*, phase P4, Fig 5).

The increased fire risk led to a renewed shift in forest management strategies that included active fire suppression (P5, Fig 5), explaining the reduction in regional FEs and below-average burning since the 1890s (Fig 4*A* and 4*H*). Foresters became firefighters, especially during the early-to-mid-19th century, and arson was an expression of anti-government resentment as historical documents indicate [68, 84]. A planned network of forest tracks to access timber from remote areas [65] was still not in place in 1845 CE (S2*B* and S2*C Fig*). Yet, it appeared as a tighter network after the major FEs in the mid-19th century (S2*D Fig*). The track network increased forest fragmentation and state regulations initiated regular cleaning of forest tracks, which successfully limited fire spread.

Fire occurrence remained low during the 20th century, despite prominent summer droughts as in the 1940s (Fig 4*C and* 4*D*). The expansion of Tuchola's forest areas from 57% in 1938 CE to 70% in 1990 CE [70] (see also the decline of HI, Fig 4*G*) due to people migrating to expanding cities and abandoning poor soils [70] was dominated by less-flammable broadleaved trees (S2 Fig), probably limiting fire occurrences.

After the 1980s, fire proxy influxes increased again (e.g., LVG, $CHAR_{300-500\mu m}$, Figs 3 and 2*H*) and MA ratios slightly decreased (i.e., more forest burning, Fig 4*I*), as confirmed by increased instrumentally-measured fire numbers and area burnt in Poland [101] (S3 Fig). HI declined strongly and pine cover increased (Figs 3*A, 4F and 4G*), which we attribute to changes in land property structures after the end of Communism. Pine monocultures increased on private lands since the 1990s, with >90% of the Tuchola forest being composed of pine today [70]. Together with increasing temperatures across central Europe during recent decades (Fig 4*B*), the fire risk has again increased [26] and possibly requires a renewed adaptation of future forest management (P6, Fig 5).

Conclusions

Our new approach provides sub-decadal records of sedimentary charcoal and intensity-specific sedimentary fire biomarkers, considering age and proxy measurement uncertainties, to assess the relative importance of specific fire regime parameters in the past (fire intensities, biomass burnt, relative fire extents, burning conditions, and fuel types) that could be included in future data-model comparisons. Compared with land cover and tree ring-based climate reconstructions, we find that since industrialization, human-driven forest management has fundamentally changed human-fire relationships.

Fire was an important land use and land management tool in the central European lowlands and globally since at least Mesolithic, and especially since Neolithic times [4, 10, 25]. The close human-forest and human-fire relationships terminated when fire was replaced by other agricultural measures [3, 5], banned from forests by state authorities, or unintendedly promoted by replacing forest with more flammable taxa, as described here for Poland. Hence, considering not only the conversion from forest to open land with increasing population densities, but also internal forest type conversions could help to improve further dynamic vegetation-fire modelling and comparisons with sedimentary proxy records that should account for several types of uncertainties.

Here, we support previous conclusions [25, 26] that the fire trends during the 19th century, as visible in global and continental charcoal compilations, were primarily influenced by humans, even before active fire suppression, closely linked with and superimposed by natural causes [15, 21, 96]. Sociopolitical shifts during industrialization could have driven unintended adaptive socio-ecological cycles that affected forest composition, fire regimes, and biogeochemical cycles [33, 34]. Timber became a precious resource, not only in Poland, and pine spread far beyond its potential natural distribution [100], similar to other highly flammable pioneer tree monocultures, such as *Eucalyptus spec.* in the subtropics and tropics (i.e., other regions of low natural flammability that were industrializing during the 18th and 19th centuries). Given these preconditions for current and future fire risks and the increased likelihood of summer droughts under future climate change [11, 12], forest management could either invest in further fire suppression measures or, by entering a new adaptive cycle, diversify monocultures to include less-flammable broadleaved taxa to prevent fire spread and further forest disturbances [26, 102, 103].

Supporting information

S1 Fig. Concept of Monte Carlo approach combing proxy and age probability density functions to statistically model robust proxy (influx) values. The Q25 to Q75 range as polygon and the median (Q50) proxy fluxes as lines in the right image.
(TIF)

S2 Fig. Regional fires in the Tuchola Forest and road network adaptation. A) Reported locations and extents of fire events in historical documents (State Archive in Gdańsk, compiled in ref. [26]). Map: 2018 OpenStreetMap and contributors, license CC-BY-SA, modified with ArcGIS Desktop: Release 10.2.2. ESRI 2014. Redlands, CA: Environmental Systems Research Institute. B-D) Historical maps with location of Czechowskie catchment (Fig 1B) indicating road network within forests: B) planned, manually drawn on the map by Prussian government authorities; C) still historical (pre-industrial) road network and D) realization of planned network (map: For better visibility and example of the tracks in forest were redrawn in pink (denser network in D than planned in B to limit fire spread). Map sources with CC-BY open access license: B) "Karte von den Provinzen Litthaen, Ost- und West-Preussen nebst dem Netzdistrict", Kart. N 1020, Blatt 92 provided by Staatsbibliothek zu Berlin—Preußischer Kulturbesitz; C) "Topographische Specialkarte des Preussischen Staats und der angrenzenden Länder (Reyman's Special-Karte)", signature PAN.C163, sheet 31 and D) "Messtischblatt" signature PAN.C633, sheet 2175; maps of C and D provided by Centralna Biblioteka Geografii I Ochrony Srodowiska IGiPZ PAN.
(TIF)

S3 Fig. Total number of fires (bars) and burned area of forests (red line) in Poland in the period 1948–2018. Data from ref. [101], Statistical Yearbook of Forestry, 2018, GUS Statistics Poland, Warsaw and Statistical data of the Polish State Fire Service KG PSP [source: www.kgpsp.gov.pl, last access: 09.08.2019].
(TIF)

S1 Code. Basic principles of CharAnalysis and Monte Carlo approach considering combined age and proxy uncertainties.
(DOCX)

Acknowledgments

Author Contributions

Conceptualization: Elisabeth Dietze, Achim Brauer, Stefan Schouten, Ellen C. Hopmans, Michał Słowiński.

Data curation: Elisabeth Dietze.

Formal analysis: Elisabeth Dietze, Dariusz Brykała, Laura T. Schreuder, Florian Ott.

Funding acquisition: Elisabeth Dietze.

Investigation: Elisabeth Dietze, Dariusz Brykała, Laura T. Schreuder, Krzysztof Jażdżewski, Milena Obremska, Anna Pieńczewska, Michał Słowiński.

Methodology: Elisabeth Dietze, Laura T. Schreuder, Michael Dietze, Ellen C. Hopmans, Michał Słowiński.

Project administration: Elisabeth Dietze.

Resources: Dariusz Brykała, Krzysztof Jażdżewski, Achim Brauer, Milena Obremska, Stefan Schouten, Ellen C. Hopmans, Michał Słowiński.

Software: Olivier Blarquez, Michael Dietze.

Supervision: Ellen C. Hopmans.

Validation: Elisabeth Dietze, Olivier Blarquez, Florian Ott, Michał Słowiński.

Visualization: Elisabeth Dietze, Dariusz Brykała.

Writing – original draft: Elisabeth Dietze.

Writing – review & editing: Elisabeth Dietze, Dariusz Brykała, Laura T. Schreuder, Olivier Blarquez, Achim Brauer, Michael Dietze, Stefan Schouten, Ellen C. Hopmans, Michał Słowiński.

References

1. Bowman DMJS Balch JK, Artaxo P Bond WJ, Carlson JM Cochrane MA, et al. Fire in the Earth System. Science. 2009; 324(5926):481–4. https://doi.org/10.1126/science.1163886 PMID: 19390038

2. Pausas JG, Keeley JE, Schwilk DW. Flammability as an ecological and evolutionary driver. Journal of Ecology. 2017; 105(2):289–97. https://doi.org/10.1111/1365-2745.12691

3. Steffen W, Persson Å, Deutsch L, Zalasiewicz J, Williams M, Richardson K, et al. The Anthropocene: From Global Change to Planetary Stewardship. AMBIO. 2011; 40(7):739. https://doi.org/10.1007/s13280-011-0185-x PMID: 22338713

4. Bowman DMJS, Balch J, Artaxo P, Bond WJ, Cochrane MA, D'Antonio CM, et al. The human dimension of fire regimes on Earth. Journal of Biogeography. 2011; 38(12):2223–36. https://doi.org/10.1111/j.1365-2699.2011.02595.x PMID: 22279247

5. Pyne SJ. Fire in the mind: Changing understandings of fire in western civilization. Philosophical transactions—Royal Society Biological sciences. 2016; 371(1696):8.

6. Kaplan JO, Krumhardt KM, Zimmermann N. The prehistoric and preindustrial deforestation of Europe. Quaternary Science Reviews. 2009; 28(27–28):3016–34. http://dx.doi.org/10.1016/j.quascirev.2009.09.028.

7. Ruddiman WF, Ellis EC, Kaplan JO, Fuller DQ. Defining the epoch we live in. Science. 2015; 348 (6230):38–9. https://doi.org/10.1126/science.aaa7297 PMID: 25838365

8. Vannière B, Blarquez O, Rius D, Doyen E, Brücher T, Colombaroli D, et al. 7000-year human legacy of elevation-dependent European fire regimes. Quaternary Science Reviews. 2016; 132:206–12. http://dx.doi.org/10.1016/j.quascirev.2015.11.012.

9. Blarquez O, Talbot J, Paillard J, Lapointe-Elmrabti L, Pelletier N, Gates St-Pierre C. Late Holocene influence of societies on the fire regime in southern Québec temperate forests. Quaternary Science Reviews. 2018; 180:63–74. https://doi.org/10.1016/j.quascirev.2017.11.022.

10. Dietze E, Theuerkauf M, Bloom K, Brauer A, Dörfler W, Feeser I, et al. Holocene fire activity during low-natural flammability periods reveals scale-dependent cultural human-fire relationships in Europe. Quaternary Science Reviews. 2018; 201:44–56. https://doi.org/10.1016/j.quascirev.2018.10.005.

11. Lhotka O, Kyselý J, Farda A. Climate change scenarios of heat waves in Central Europe and their uncertainties. Theoretical and Applied Climatology. 2018; 131(3):1043–54. https://doi.org/10.1007/s00704-016-2031-3

12. IPCC. Climate Change 2014: Impacts, Adaptation, and Vulnerability. Part B: Regional Aspects. Contribution of Working Group II to the Fifth Assessment Report of the Intergovernmental Panel on Climate Change [Barros V.R., Field C.B., Dokken D.J., Mastrandrea M.D., Mach K.J., Bilir T.E., Chatterjee M., Ebi K.L., Estrada Y.O., Genova R.C., Girma B., Kissel E.S., Levy A.N., MacCracken S., Mastrandrea P.R., and White L.L. (eds.)]. Cambridge, United Kingdom and New York, NY, USA: Cambridge University Press; 2014. 688 p.

13. Munteanu C, Kuemmerle T, Keuler NS, Müller D, Balázs P, Dobosz M, et al. Legacies of 19th century land use shape contemporary forest cover. Global Environmental Change. 2015; 34:83–94. https://doi.org/10.1016/j.gloenvcha.2015.06.015.

14. van der Werf GR, Peters W, van Leeuwen TT, Giglio L. What could have caused pre-industrial biomass burning emissions to exceed current rates? Clim Past. 2013; 9(1):289–306. https://doi.org/10.5194/cp-9-289-2013

15. Marlon JR, Bartlein PJ, Carcaillet C, Gavin DG, Harrison SP, Higuera PE, et al. Climate and human influences on global biomass burning over the past two millennia. Nature Geosci. 2008; 1(10):697–702. http://www.nature.com/ngeo/journal/v1/n10/suppinfo/ngeo313_S1.html.

16. Taylor AH, Trouet V, Skinner CN, Stephens S. Socioecological transitions trigger fire regime shifts and modulate fire–climate interactions in the Sierra Nevada, USA, 1600–2015 CE. Proceedings of the National Academy of Sciences. 2016; 113(48):13684–9. https://doi.org/10.1073/pnas.1609775113 PMID: 27849589

17. Power M, Mayle F, Bartlein P, Marlon J, Anderson R, Behling H, et al. Climatic control of the biomass-burning decline in the Americas after ad 1500. The Holocene. 2013; 23(1):3–13. https://doi.org/10.1177/0959683612450196

18. Wang Z, Chappellaz J, Park K, Mak JE. Large Variations in Southern Hemisphere Biomass Burning During the Last 650 Years. Science. 2010. https://doi.org/10.1126/science.1197257 PMID: 21127215

19. Ferretti DF, Miller JB, White JWC, Etheridge DM, Lassey KR, Lowe DC, et al. Unexpected Changes to the Global Methane Budget over the Past 2000 Years. Science. 2005; 309(5741):1714–7. https://doi.org/10.1126/science.1115193 PMID: 16151008

20. Marlon JR, Kelly R, Daniau AL, Vannière B, Power MJ, Bartlein P, et al. Reconstructions of biomass burning from sediment-charcoal records to improve data–model comparisons. Biogeosciences. 2016; 13(11):3225–44. https://doi.org/10.5194/bg-13-3225-2016

21. Molinari C, Lehsten V, Bradshaw RHW, Power MJ, Harmand P, Arneth A, et al. Exploring potential drivers of European biomass burning over the Holocene: a data-model analysis. Global Ecology and Biogeography. 2013; 22(12):1248–60. https://doi.org/10.1111/geb.12090

22. Pechony O, Shindell DT. Driving forces of global wildfires over the past millennium and the forthcoming century. Proceedings of the National Academy of Sciences. 2010; 107(45):19167–70. https://doi.org/10.1073/pnas.1003669107 PMID: 20974914

23. Marcisz K, Gałka M, Pietrala P, Miotk-Szpiganowicz G, Obremska M, Tobolski K, et al. Fire activity and hydrological dynamics in the past 5700 years reconstructed from Sphagnum peatlands along the oceanic–continental climatic gradient in northern Poland. Quaternary Science Reviews. 2017; 177:145–57. https://doi.org/10.1016/j.quascirev.2017.10.018.

24. Marcisz K, Colombaroli D, Jassey VEJ, Tinner W, Kołaczek P, Gałka M, et al. A novel testate amoebae trait-based approach to infer environmental disturbance in Sphagnum peatlands. Scientific Reports. 2016; 6:33907. https://doi.org/10.1038/srep33907 https://www.nature.com/articles/srep33907#supplementary-information. PMID: 27658521

25. McWethy DB, Higuera PE, Whitlock C, Veblen TT, Bowman DMJS, Cary GJ, et al. A conceptual framework for predicting temperate ecosystem sensitivity to human impacts on fire regimes. Global Ecology and Biogeography. 2013; 22(8):900–12. https://doi.org/10.1111/geb.12038

26. Słowiński M, Lamentowicz M, Łucóv D, Barabach J, Brykała D, Tyszkowski S, et al. Paleoecological and historical data as an important tool in ecosystem management. Journal of Environmental Management. 2019; 236:755–68. https://doi.org/10.1016/j.jenvman.2019.02.002 PMID: 30776550

27. Balch JK, Bradley BA, Abatzoglou JT, Nagy RC, Fusco EJ, Mahood AL. Human-started wildfires expand the fire niche across the United States. Proceedings of the National Academy of Sciences. 2017; 114(11):2946–51. https://doi.org/10.1073/pnas.1617394114 PMID: 28242690

28. van Marle MJE, Kloster S, Magi BI, Marlon JR, Daniau AL, Field RD, et al. Historic global biomass burning emissions for CMIP6 (BB4CMIP) based on merging satellite observations with proxies and fire models (1750–2015). Geosci Model Dev. 2017; 10(9):3329–57. https://doi.org/10.5194/gmd-10-3329-2017

29. Stephens SL, Agee JK, Fulé PZ, North MP, Romme WH, Swetnam TW, et al. Managing Forests and Fire in Changing Climates. Science. 2013; 342(6154):41–2. https://doi.org/10.1126/science.1240294 PMID: 24092714

30. Keane RE. Wildland Fuel Fundamentals and Applications. New York, NY: Springer; 2015.

31. Andela N, Morton DC, Giglio L, Chen Y, van der Werf GR, Kasibhatla PS, et al. A human-driven decline in global burned area. Science. 2017; 356(6345):1356–62. https://doi.org/10.1126/science.aal4108 PMID: 28663495

32. Whitlock C, Colombaroli D, Conedera M, Tinner W. Land-use history as a guide for forest conservation and management. Conservation Biology. 2018; 32(1):84–97. https://doi.org/10.1111/cobi.12960 PMID: 28574184

33. Arneth A, Sitch S, Pongratz J, Stocker BD, Ciais P, Poulter B, et al. Historical carbon dioxide emissions caused by land-use changes are possibly larger than assumed. Nature Geosci. 2017; 10(2):79–84. https://doi.org/10.1038/ngeo2882 http://www.nature.com/ngeo/journal/v10/n2/abs/ngeo2882.html#supplementary-information.

34. Ward DS, Shevliakova E, Malyshev S, Rabin S. Trends and Variability of Global Fire Emissions Due To Historical Anthropogenic Activities. Global Biogeochemical Cycles. 2018; 32(1):122–42. https://doi.org/10.1002/2017GB005787

35. Keeley JE. Fire intensity, fire severity and burn severity: a brief review and suggested usage. International Journal of Wildland Fire. 2009; 18(1):116–26. https://doi.org/10.1071/WF07049.

36. Han YM, Peteet DM, Arimoto R, Cao JJ, An ZS, Sritrairat S, et al. Climate and Fuel Controls on North American Paleofires: Smoldering to Flaming in the Late-glacial-Holocene Transition. Scientific Reports. 2016; 6:20719. https://doi.org/10.1038/srep20719 http://www.nature.com/articles/srep20719#supplementary-information. PMID: 26860820

37. Legrand M, McConnell J, Fischer H, Wolff EW, Preunkert S, Arienzo M, et al. Boreal fire records in Northern Hemisphere ice cores: a review. Clim Past. 2016; 12(10):2033–59. https://doi.org/10.5194/cp-12-2033-2016

38. Tinner W, Hofstetter S, Zeugin F, Conedera M, Wohlgemuth T, Zimmermann L, et al. Long-distance transport of macroscopic charcoal by an intensive crown fire in the Swiss Alps—implications for fire history reconstruction. The Holocene. 2006; 16(2):287–92. https://doi.org/10.1191/0959683606hl925rr

39. Peters ME, Higuera PE. Quantifying the source area of macroscopic charcoal with a particle dispersal model. Quaternary Research. 2007; 67(2):304–10. http://dx.doi.org/10.1016/j.yqres.2006.10.004.

40. Akagi SK, Yokelson RJ, Wiedinmyer C, Alvarado MJ, Reid JS, Karl T, et al. Emission factors for open and domestic biomass burning for use in atmospheric models. Atmos Chem Phys. 2011; 11(9):4039–72. https://doi.org/10.5194/acp-11-4039-2011

41. Hawthorne D, Courtney Mustaphi CJ, Aleman JC, Blarquez O, Colombaroli D, Daniau A-L, et al. Global Modern Charcoal Dataset (GMCD): A tool for exploring proxy-fire linkages and spatial patterns of biomass burning. Quaternary International. 2018; 488:3–17. https://doi.org/10.1016/j.quaint.2017.03.046.

42. Higuera PE, Brubaker LB, Anderson PM, Hu FS, Brown TA. Vegetation mediated the impacts of post-glacial climate change on fire regimes in the south-central Brooks Range, Alaska. Ecological Monographs. 2009; 79(2):201–19. https://doi.org/10.1890/07-2019.1

43. Conedera M, Tinner W, Neff C, Meurer M, Dickens AF, Krebs P. Reconstructing past fire regimes: methods, applications, and relevance to fire management and conservation. Quaternary Science Reviews. 2009; 28(5–6):555–76. http://dx.doi.org/10.1016/j.quascirev.2008.11.005.

44. Whitlock C, Larsen C. Charcoal as a Fire Proxy. In: Smol JP, Birks HJB, Last WM, editors. Tracking Environmental Change Using Lake Sediments Terrestrial, Algal, and Siliceous Indicators. 3. Dordrecht, The Netherlands: KluwerAcademic Publishers; 2001. p. 75–97.

45. Marcisz K, Tinner W, Colombaroli D, Kolaczek P, Słowiński M, Fiaikiewicz-Koziel B, et al. Long-term hydrological dynamics and fire history over the last 2000 years in CE Europe reconstructed from a high-resolution peat archive. Quaternary Science Reviews. 2015; 112:138–52. https://doi.org/10.1016/j.quascirev.2015.01.019 WOS:000351977500011.

46. Kuo L-J, Herbert BE, Louchouarn P. Can levoglucosan be used to characterize and quantify char/charcoal black carbon in environmental media? Organic Geochemistry. 2008; 39(10):1466–78. http://doi.org/10.1016/j.orggeochem.2008.04.026.

47. Simoneit BRT, Schauer JJ, Nolte CG, Oros DR, Elias VO, Fraser MP, et al. Levoglucosan, a tracer for cellulose in biomass burning and atmospheric particles. Atmospheric Environment. 1999; 33(2):173–82. http://dx.doi.org/10.1016/S1352-2310(98)00145-9.

48. Schmidl C, Marr IL, Caseiro A, Kotianová P, Berner A, Bauer H, et al. Chemical characterisation of fine particle emissions from wood stove combustion of common woods growing in mid-European Alpine regions. Atmospheric Environment. 2008; 42(1):126–41. https://doi.org/10.1016/j.atmosenv.2007.09.028.

49. Fabbri D, Torri C, Simoneit BRT, Marynowski L, Rushdi AI, Fabiańska MJ. Levoglucosan and other cellulose and lignin markers in emissions from burning of Miocene lignites. Atmospheric Environment. 2009; 43(14):2286–95. https://doi.org/10.1016/j.atmosenv.2009.01.030

50. Kuo L-J, Louchouarn P, Herbert BE. Influence of combustion conditions on yields of solvent-extractable anhydrosugars and lignin phenols in chars: Implications for characterizations of biomass combustion residues. Chemosphere. 2011; 85(5):797–805. https://doi.org/10.1016/j.chemosphere.2011.06.074 PMID: 21762951

51. Engling G, Carrico CM, Kreidenweis SM, Collett JL Jr, Day DE, Malm WC, et al. Determination of levoglucosan in biomass combustion aerosol by high-performance anion-exchange chromatography with pulsed amperometric detection. Atmospheric Environment. 2006; 40(SUPPL. 2):299–311. https://doi.org/10.1016/j.atmosenv.2005.12.069

52. Schüpbach S, Kirchgeorg T, Colombaroli D, Beffa G, Radaelli M, Kehrwald NM, et al. Combining charcoal sediment and molecular markers to infer a Holocene fire history in the Maya Lowlands of Petén, Guatemala. Quaternary Science Reviews. 2015; 115(0):123–31. http://dx.doi.org/10.1016/j.quascirev.2015.03.004.

53. Battistel D, Argiriadis E, Kehrwald N, Spigariol M, Russell JM, Barbante C. Fire and human record at Lake Victoria, East Africa, during the Early Iron Age: Did humans or climate cause massive ecosystem changes? The Holocene. 2017; 27(7):997–1007. https://doi.org/10.1177/0959683616678466

54. Argiriadis E, Battistel D, McWethy DB, Vecchiato M, Kirchgeorg T, Kehrwald NM, et al. Lake sediment fecal and biomass burning biomarkers provide direct evidence for prehistoric human-lit fires in New Zealand. Scientific Reports. 2018; 8(1):12113. https://doi.org/10.1038/s41598-018-30606-3 PMID: 30108240

55. Sang XF, Gensch I, Kammer B, Khan A, Kleist E, Laumer W, et al. Chemical stability of levoglucosan: An isotopic perspective. Geophysical Research Letters. 2016; 43(10):5419–24. https://doi.org/10.1002/2016GL069179

56. Fraser MP, Lakshmanan K. Using Levoglucosan as a Molecular Marker for the Long-Range Transport of Biomass Combustion Aerosols. Environmental Science & Technology. 2000; 34(21):4560–4. https://doi.org/10.1021/es991229l

57. Mullaugh KM, Byrd JN, Avery GB Jr, Mead RN, Willey JD, Kieber RJ. Characterization of carbohydrates in rainwater from the Southeastern North Carolina. Chemosphere. 2014; 107:51–7. https://doi.org/10.1016/j.chemosphere.2014.03.014 PMID: 24875870

58. Knicker H, Hilscher A, de la Rosa JM, González-Pérez JA, González-Vila FJ. Modification of biomarkers in pyrogenic organic matter during the initial phase of charcoal biodegradation in soils. Geoderma. 2013;197–198:43–50. http://dx.doi.org/10.1016/j.geoderma.2012.12.021.

59. Schreuder LT, Hopmans EC, Stuut J-BW, Sinninghe Damsté JS, Schouten S. Transport and deposition of the fire biomarker levoglucosan across the tropical North Atlantic Ocean. Geochimica et Cosmochimica Acta. 2018. https://doi.org/10.1016/j.gca.2018.02.020.

60. Wójcik G, Marciniak K. Opady atmosferyczne w regionie Dolnej Wisły w okresie 1951–1980 [Atmospheric precipitation in the Lower Vistula region in the period 1951–1980]. In: Churski Z, editor. Uwarunkowania przyrodnicze i społeczno-ekonomiczne zagospodarowania Dolnej Wisły [Natural and socio-economic conditions of the Lower Vistula menagement]. Toruń: IG UMK; 1993. p. 107–21.

61. Woś A. Klimat Polski [Climate of Poland]. Warszawa: PWN; 1999.

62. Archibald S, Lehmann CER, Gómez-Dans JL, Bradstock RA. Defining pyromes and global syndromes of fire regimes. Proceedings of the National Academy of Sciences. 2013; 110(16):6442–7. https://doi.org/10.1073/pnas.1211466110 PMID: 23559374

63. San-Miguel-Ayanz J, Schulte E, Schmuck G, Camia A, Strobl P, Libertà G, et al. Comprehensive monitoring of wildfires in Europe: the European Forest Fire Information System (EFFIS). In: Tiefenbacher J, editor. Approaches to Managing Disaster—Assessing Hazards, Emergencies and Disaster Impacts. http://effis.jrc.ec.europa.eu/:InTech; 2012.

64. Niklasson M, Zin E, Zielonka T, Feijen M, Korczyk AF, Churski M, et al. A 350-year tree-ring fire record from Białowieża Primeval Forest, Poland: implications for Central European lowland fire history. Journal of Ecology. 2010; 98(6):1319–29. https://doi.org/10.1111/j.1365-2745.2010.01710.x

65. Broda J. Historia leśnictwa w Polsce [History of forestry in Poland]. Poznań: Wydawnictwo Akademii Rolniczej im Augusta Cieszkowskiego w Poznaniu; 2000.

66. McGrath MJ, Luyssaert S, Meyfroidt P, Kaplan JO, Bürgi M, Chen Y, et al. Reconstructing European forest management from 1600 to 2010. Biogeosciences. 2015; 12(14):4291–316. https://doi.org/10.5194/bg-12-4291-2015

67. Bienias D. Las i człowiek w Borach Tucholskich (uwagi o bartnictwie i smolarstwie w Borach Tucholskich) [The Forest and human in the Tuchola Pinewoods (comments about forest beekeeping and tar burning)]. In: Woźny J, editor. Dziedzictwo techniczne Borów Tucholskich Bydgoszcz: Przedsiębiorstwo Marketingowe LOGO; 2009. p. 43–51.

68. Hasel K, Schwartz E. Forstgeschichte. Ein Grundriss für Studium und Praxis [Forest history. A sketch for study and application]. 2nd ed. Remagen: Kessel; 2002.

69. Konig A. Die Entwicklung der staatlichen Forstwirtschaft in Westpreussen und ihre Beziehungen zur Landeskultur [The development of governmental forestry in Western Prussia and its relationship to state culture]. Gdansk1905.

70. Giętkowski T. Zmiany lesistości Borów Tucholskich w latach 1938–2000 [Temporal change of forest area in Tuchola Pinewoods region between 1938–2000]. Promotio Geographica Bydgostiensia. 2009; 4.

71. Słowiński M, Błaszkiewicz M, Brauer A, Noryśkiewicz B, Ott F, Tyszkowski S. The role of melting dead ice on landscape transformation in the early Holocene in Tuchola Pinewoods, North Poland. Quaternary International. 2015; 388:64–75. http://dx.doi.org/10.1016/j.quaint.2014.06.018.

72. Ott F, Kramkowski M, Wulf S, Plessen B, Serb J, Tjallingii R, et al. Site-specific sediment responses to climate change during the last 140 years in three varved lakes in Northern Poland. The Holocene. 2018; 28(3):464–77. https://doi.org/10.1177/0959683617729448

73. Trachsel M, Telford RJ. All age–depth models are wrong, but are getting better. The Holocene. 2017; 27(6):860–9. https://doi.org/10.1177/0959683616675939

74. Clark JS. Particle motion and the theory of charcoal analysis: Source area, transport, deposition, and sampling. Quaternary Research. 1988; 30(1):67–80. http://dx.doi.org/10.1016/0033-5894(88)90088-9.

75. Hopmans EC, dos Santos RAL, Mets A, Damsté JSS, Schouten S. A novel method for the rapid analysis of levoglucosan in soils and sediments. Organic geochemistry. 2013; 58:86–8.

76. Theuerkauf M, Couwenberg J, Kuparinen A, Liebscher V. A matter of dispersal: REVEALSinR introduces state-of-the-art dispersal models to quantitative vegetation reconstruction. Veget Hist Archaeobot. 2016:1–13. https://doi.org/10.1007/s00334-016-0572-0

77. Blarquez O, Girardin MP, Leys B, Ali AA, Aleman JC, Bergeron Y, et al. Paleofire reconstruction based on an ensemble-member strategy applied to sedimentary charcoal. Geophysical Research Letters. 2013; 40(11):2667–72. https://doi.org/10.1002/grl.50504

78. Ali AA, Blarquez O, Girardin MP, Hély C, Tinquaut F, El Guellab A, et al. Control of the multimillennial wildfire size in boreal North America by spring climatic conditions. Proceedings of the National Academy of Sciences. 2012; 109(51):20966–70. https://doi.org/10.1073/pnas.1203467109 PMID: 23213207

79. Higuera PE, Chipman ML, Barnes JL, Urban MA, Hu FS. Variability of tundra fire regimes in Arctic Alaska: millennial-scale patterns and ecological implications. Ecological Applications. 2011; 21 (8):3211–26. https://doi.org/10.1890/11-0387.1

80. Loader C. locfit: Local Regression, Likelihood and Density Estimation. R package. 1.5–9.1. ed2013.

81. Young D, Benaglia T, Chauveau D, Hunter D. mixtools: Tools for Analyzing Finite Mixture Models. R package. 1.1.0 ed2017.

82. Higuera PE, Brubaker LB, Anderson PM, Brown TA, Kennedy AT, Hu FS. Frequent Fires in Ancient Shrub Tundra: Implications of Paleorecords for Arctic Environmental Change. PLOS ONE. 2008; 3(3): e0001744. https://doi.org/10.1371/journal.pone.0001744 PMID: 18320025

83. Gavin DG, Hu FS, Lertzman K, Corbett P. Weak climatic control of stand-scale fire history during the late Holocene. Ecology. 2006; 87(7):1722–32. https://doi.org/10.1890/0012-9658(2006)87[1722:wccosf]2.0.co;2 PMID: 16922322

84. Schütte R. Die Tucheler Haide vornehmlich in forstlicher Beziehung. Danzig: 1893.

85. Clark JS, Royall PD. Pre-industrial particulate emissions and carbon sequestration from biomass burning in North America. Biogeochemistry. 1994; 24(1):35–51. https://doi.org/10.1007/bf00001306

86. Higuera PE, Peters ME, Brubaker LB, Gavin DG. Understanding the origin and analysis of sediment-charcoal records with a simulation model. Quaternary Science Reviews. 2007; 26(13–14):1790–809. http://dx.doi.org/10.1016/j.quascirev.2007.03.010.

87. Adolf C, Wunderle S, Colombaroli D, Weber H, Gobet E, Heiri O, et al. The sedimentary and remote-sensing reflection of biomass burning in Europe. Global Ecology and Biogeography. 2018; 27(2):199–212. https://doi.org/10.1111/geb.12682

88. Vachula RS, Russell JM, Huang Y, Richter N. Assessing the spatial fidelity of sedimentary charcoal size fractions as fire history proxies with a high-resolution sediment record and historical data. Palaeo-geography, Palaeoclimatology, Palaeoecology. 2018; 508:166–75. https://doi.org/10.1016/j.palaeo.2018.07.032

89. Cyzman W, Oleksik-Tusińska A. Jednolity program gospodarczo–ochronny dla leśnego kompleksu promocyjnego „Bory Tucholskie" [Unified economic and protective programm for Promotional Forest Complex "Tuchola Pinewoods"]. Torun2008. 233 p.

90. Geissler A, Koschinski K. 130 Jahre "Ostbahn Berlin—Königsberg—Baltikum". Berlin: GVE; 1997.

91. Büntgen U, Tegel W, Nicolussi K, McCormick M, Frank D, Trouet V, et al. 2500 Years of European Climate Variability and Human Susceptibility. Science. 2011; 331(6017):578–82. https://doi.org/10.1126/science.1197175 PMID: 21233349

92. Cook ER, Seager R, Kushnir Y, Briffa KR, Büntgen U, Frank D, et al. Old World megadroughts and pluvials during the Common Era. Science Advances. 2015; 1(10). https://doi.org/10.1126/sciadv.1500561 PMID: 26601136

93. Miętus M. Jednorodność wieloletnich serii pomiarowych. Rzeczywistość czy fikcja? Annales Universitatis Mariae Curie-Skłodowska Sectio B 2000/2001; 50/51(29):239–48.

94. Zumbrunnen T, Bugmann H, Conedera M, Bürgi M. Linking Forest Fire Regimes and Climate—A Historical Analysis in a Dry Inner Alpine Valley. Ecosystems. 2009; 12(1):73–86. https://doi.org/10.1007/s10021-008-9207-3

95. Christian HJ, Blakeslee RJ, Boccippio DJ, Boeck WL, Buechler DE, Driscoll KT, et al. Global frequency and distribution of lightning as observed from space by the Optical Transient Detector. Journal of Geophysical Research: Atmospheres. 2003; 108(D1):ACL 4-1-ACL 4–15. https://doi.org/10.1029/2002JD002347

96. Roos CI, Zedeño MN, Hollenback KL, Erlick MMH. Indigenous impacts on North American Great Plains fire regimes of the past millennium. Proceedings of the National Academy of Sciences. 2018; 115(32):8143–8. https://doi.org/10.1073/pnas.1805259115 PMID: 30037995

97. Dost P. 100 Jahre Königliche Ostbahn in Berlin [100 years of the Royal East Railway in Berlin]. West-preußen-Jahrbuch. 1967; 17:83–8.

98. Trollope WSW, Trollope LA, Hartnett DC. Fire behaviour as a key factor in the fire ecology of African grasslands and savannas. In: Viegas DX, editor. Forest Fire Research and Wildland Fire: Millpress, Rotterdam Netherlands; 2002.

99. Gunderson LH, Holling CS. Panarchy: Understanding Transformations In Human And Natural Systems. Washington, D.C.: Island Press; 2002.

100. Houston Durrant T, de Rigo D, Caudullo G. Pinus sylvestris in Europe: distribution, habitat, usage and threats. In: San-Miguel-Ayanz J, de Rigo D, Caudullo G, Houston Durrant T, Mauri A, editors. European Atlas of Forest Tree Species. Luxembourg: Publications Office of the European Union; 2016. p. e016b94+.

101. Szczygieł R. Pożary w lasach–charakterystyka, przyczyny, koszty [Fires in the forests–characteristics, drivers, costs]. In: Guzewski P, Wróblewski D, Małozięć D, editors. Czerwona księga pożarów [Red book of fires]. 1. Józefów: Wydawnictwo CNBOP-PIB; 2016. p. 463–510.

102. Girardin MP, Ali AA, Carcaillet C, Blarquez O, Hély C, Terrier A, et al. Vegetation limits the impact of a warm climate on boreal wildfires. New Phytologist. 2013; 199(4):1001–11. https://doi.org/10.1111/nph.12322 PMID: 23691916

103. Seidl R, Thom D, Kautz M, Martin-Benito D, Peltoniemi M, Vacchiano G, et al. Forest disturbances under climate change. Nature Clim Change. 2017; 7(6):395–402. https://doi.org/10.1038/nclimate3303 http://www.nature.com/nclimate/journal/v7/n6/abs/nclimate3303.html#supplementary-information. PMID: 28861124